Time-Dependent Inhibition of recA Protein-Catalyzed ATP Hydrolysis by ATPγS: Evidence for a Rate-Determining Isomerization of the recA−ssDNA Complex[†]

Brian F. Paulus and Floyd R. Bryant*

Department of Biochemistry, The Johns Hopkins University, School of Public Health, Baltimore, Maryland 21205

Received March 13, 1997[⊗]

ABSTRACT: The ATP analog ATPγS is a competitive inhibitor of the recA protein-catalyzed ssDNA-dependent ATP hydrolysis reaction. The degree of inhibition by ATPγS, however, changes in a time-dependent manner and is consistent with a two step binding mechanism. In the first step, ATPγS binds to the recA−ssDNA complex in a rapid equilibrium step (K_D = 50 μM). This initial binding step is followed by an isomerization of the recA−ssDNA−ATPγS complex to a new conformational state in which ATPγS is bound with a significantly higher affinity (overall K_D = 0.3 μM). This isomerization is followed by the slow hydrolysis of ATPγS to ADP and thiophosphate (0.01 min^{-1}). The first-order rate constant for the ATPγS-mediated isomerization step (20 min^{-1}), although significantly greater than the rate of ATPγS hydrolysis, is identical to the steady-state rate constant for the recA protein-catalyzed ATP hydrolysis reaction. These results are consistent with a kinetic model in which an ATP-mediated isomerization of the recA−ssDNA complex represents the rate-determining step on the recA protein-catalyzed ssDNA-dependent ATP hydrolysis reaction pathway.

The recA protein of *Escherichia coli* (M_r 37 842; 352 amino acids) is essential for homologous genetic recombination and for the postreplicative repair of damaged DNA. The purified recA protein promotes a variety of DNA strand exchange reactions that presumably reflect *in vivo* recombination functions. The most extensively investigated DNA pairing reaction is the ATP-dependent three-strand exchange reaction, in which a circular ssDNA[1] molecule and a homologous linear dsDNA molecule are recombined to yield a nicked circular dsDNA molecule and a linear ssDNA molecule. This reaction proceeds in three phases. In the first phase, the circular ssDNA substrate is coated with recA protein to form a presynaptic complex; this complex will catalyze the hydrolysis of ATP to ADP and P_i. In the second phase, the presynaptic complex interacts with a dsDNA molecule, the homologous sequences are brought into register, and pairing between the circular ssDNA and the complementary strand from the dsDNA is initiated. In the third phase, the complementary linear strand is completely transferred to the circular ssDNA by unidirectional branch migration to yield the nicked circular dsDNA and displaced linear ssDNA products (Roca & Cox, 1990; Kowalczykowski, 1991).

The presynaptic complex formed between the recA protein and ssDNA is the active recombinational entity in DNA strand exchange reactions. The recA protein binds cooperatively to ssDNA, forming a right-handed helical protein filament with one recA monomer per three nucleotides of ssDNA and six recA monomers per turn of the filament. In the absence of nucleotide cofactor or in the presence of ADP, the helical filament exists in a "collapsed" or "closed" conformation (helical pitch 65 Å) and is inactive in strand exchange. In the presence of ATP, however, the filament isomerizes to an "extended" or "open" conformation (helical pitch 95 Å) and is active in strand exchange (Egelman, 1993).

The ATP analog ATPγS has been widely used to investigate the mechanism of action of the recA protein. Although the steady-state turnover number for recA protein-catalyzed ssDNA-dependent ATPγS hydrolysis (0.01 min^{-1}) is approximately 2000-fold lower than that for the hydrolysis of ATP (20 min^{-1}), the recA−ssDNA complex does isomerize to the open conformation and is active in strand exchange in the presence of ATPγS, suggesting that nucleotide hydrolysis may not be absolutely required for these processes (Roca & Cox, 1990; Kowalczykowski, 1991). ATP hydrolysis, however, has been shown to be required in order for the strand exchange reaction to proceed in a unidirectional manner, to permit the strand exchange reaction to proceed past lesions, mismatches, and heterologous inserts, and to promote the dissociation of recA protein from the DNA products after the strand exchange reaction has been completed (Cox, 1994). It is likely that the poorly hydrolyzed ATPγS traps the recA−ssDNA complex in a conformational state that is analogous to the state that exists after ATP has bound but before it is hydrolyzed.

In order to monitor the conformational transitions of the recA protein directly, we recently constructed a mutant recA protein in which His163 was replaced by a tryptophan reporter group. The [H163W]recA protein catalyzes ATP hydrolysis with the same turnover number as the wild-type protein (18−20 min^{-1}), has an $S_{0.5}$(ATP) value (70 μM) that is similar to that for the wild-type protein (45 μM), and is fully functional in the three-strand exchange reaction.[2] In addition, the fluorescence of the Trp163 reporter group is very sensitive to the binding of ATP and ATPγS to the

[†] This work was supported by Grant GM 36516 from the National Institutes of Health.

* Author to whom correspondence should be addressed. Telephone: 410-955-3895. Fax: 410-955-2926.

[⊗] Abstract published in *Advance ACS Abstracts,* June 1, 1997.

[1] Abbreviations: ssDNA, single-stranded DNA; dsDNA, double-stranded DNA; ATPγS, adenosine 5′-*O*-(thiotriphosphate).

[2] $S_{0.5}$ is the substrate concentration required for half-maximal velocity.

S0006-2960(97)00576-X CCC: $14.00

[H163W]recA−ssDNA complex (Stole & Bryant, 1994, 1995). The pre-steady-state kinetics of the ATP-mediated fluorescence change were consistent with a two-step binding mechanism in which an initial rapid equilibrium binding of ATP to the recA−ssDNA complex is followed by a first-order isomerization of the complex to a new conformational state. The rate constant for the isomerization step (18 min^{-1}) was identical to the steady-state turnover number for ATP hydrolysis, suggesting that the isomerization was the rate-determining step on the ATP hydrolysis reaction pathway. The kinetics of the ATPγS-mediated fluorescence change were also consistent with a two-step binding mechanism with a unimolecular isomerization of 18 min^{-1}. Since ATPγS was not hydrolyzed appreciably on the time scale of these experiments (0.01 min^{-1}), this indicated that the isomerization step follows ATPγS (or ATP) binding but precedes ATPγS (or ATP) hydrolysis (Stole & Bryant, 1997).

The kinetic model described above was based entirely on the observation of time-dependent changes in the fluorescence properties of the [H163W]recA−ssDNA complex that occurred after addition of ATP or ATPγS. In order to directly correlate these fluorescence changes with the actual states of the recA−ssDNA complex, we examined the effect of ATPγS on the kinetics of the ATP hydrolysis reaction. If the two-step binding mechanism is correct, our model predicts that ATPγS should be a competitive inhibitor of ATP hydrolysis, and that the degree of inhibition by ATPγS should increase in a time-dependent manner as the recA−ssDNA−ATPγS complex isomerizes from the initial state (in which ATPγS is less tightly bound) to the second conformational state (in which ATPγS is more tightly bound). The results of our kinetic study are presented in this report.

EXPERIMENTAL PROCEDURES

Materials. Wild-type and [H163W]recA proteins were prepared as described previously (Bryant, 1988; Stole & Bryant, 1994). ATP was from Pharmacia, and ATPγS was from Sigma. [α-^{32}P]ATP and [γ-^{35}S]ATPγS were from Amersham. dT_{50} DNA was from Gibco BRL. All DNA concentrations are expressed as total nucleotides.

ATP Hydrolysis Assay. ATP and ATPγS hydrolysis was measured using a thin-layer chromatography method as previously described (Weinstock et al., 1979). Specific reaction conditions are given in the relevant figure legends.

Data Analysis. The kinetic simulations in this report were produced using the KINSIM program (Frieden, 1993). Initially, preliminary simulations were generated using kinetic parameters derived for an analogous reaction scheme in our recent transient fluorescence studies of the [H163W]recA protein ($K_1 = 90\ \mu$M, $K_3 = 70\ \mu$M, $k_2 = 18\ min^{-1}$, $k_4 = 16\ min^{-1}$, and $k_{-4} = 2\ min^{-1}$; Stole & Bryant, 1997), and the value $k_{-2} = 0.13\ min^{-1}$ determined here (see Results). These parameters were then adjusted to give the best overall fit of the kinetic model to each data set. The final parameters that were used for each set of kinetic simulations are given in the relevant figure legends.

RESULTS

Time-Dependent Change in the Inhibition of ATP Hydrolysis by ATPγS. The ssDNA-dependent recA protein-catalyzed hydrolysis of ATP was measured in the presence and absence of ATPγS. The reaction solutions contained recA protein (1 μM) and a saturating concentration of dT_{50} (20 μM).[3] All of the kinetic experiments reported below were carried out with our mutant [H163W]recA protein so that the results could be related directly to our recent transient fluorescence studies (see the introduction; Stole & Bryant, 1997). In all cases, however, equivalent kinetic results were obtained with the wild-type recA protein (data not shown). All reactions were carried out at pH 7.5 and 37 °C.

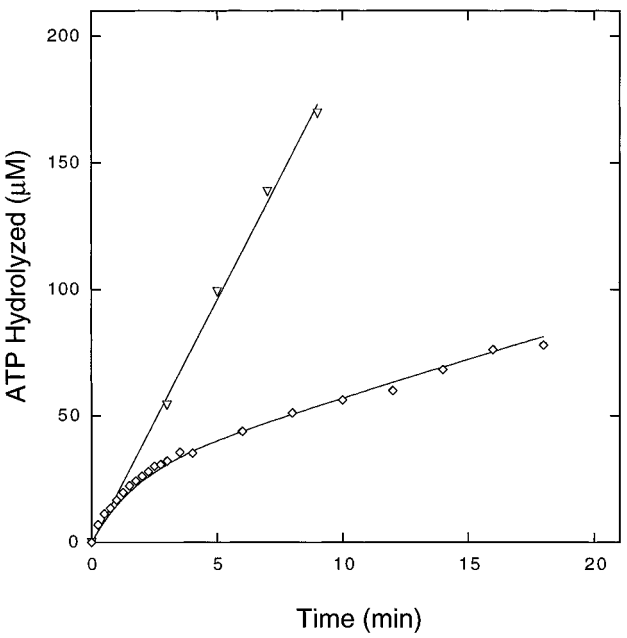

FIGURE 1: Time-dependent inhibition of recA protein-catalyzed ssDNA-dependent ATP hydrolysis by ATPγS. Reaction solutions contained 25 mM Tris-HCl (pH 7.5), 10 mM $MgCl_2$, 20 μM dT_{50}, 1 μM [H163W]recA protein, 1 mM [α-^{32}P]ATP, and either 0 μM (▽) or 20 μM ATPγS (◇). The reactions were initiated by the simultaneous addition of ATP and ATPγS after incubation of all other components for 8 min at 37 °C. The points represent ATP hydrolyzed as a function of time at 37 °C. The solid line was calculated using the mechanism in Scheme 1 and the parameters $K_1 = 55\ \mu$M, $K_3 = 75\ \mu$M, $k_2 = 20\ min^{-1}$, $k_{-2} = 0.1\ min^{-1}$, $k_4 = 20.5\ min^{-1}$, and $k_{-4} = 2\ min^{-1}$.

Time courses of ATP hydrolysis that were obtained at a saturating concentration of ATP [1 mM; $S_{0.5}$(ATP) = 70 μM] and in the absence or presence of ATPγS (20 μM) are shown in Figure 1. These reactions were initiated by adding ATP and ATPγS simultaneously to a reaction solution which contained preformed recA−ssDNA complex. In the absence of ATPγS, the ATP hydrolysis reaction followed a linear time course with the expected steady-state rate constant of 20 min^{-1} (Stole & Bryant, 1994). In the presence of ATPγS, however, a nonlinear time course was observed. At early time points (<1 min), the rate of ATP hydrolysis was nearly the same as that measured in the absence of ATPγS. As the reaction progressed, however, the rate of ATP hydrolysis decreased until it reached a new steady-state rate that was significantly lower than that measured in the absence of ATPγS.

The nonlinear time course shown in Figure 1 indicated that the degree of inhibition of the ATP hydrolysis reaction by ATPγS was changing in a time-dependent manner. This kinetic behavior was consistent with the mechanism shown

[3] dT_{50} is the smallest ssDNA that will maximally activate the ATP hydrolysis activity of the recA protein (Brenner et al., 1987).

Scheme 1

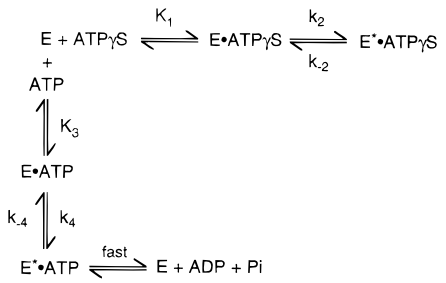

in Scheme 1. In this mechanism, both ATP and ATPγS bind to the recA−ssDNA complex (designated E) in a rapid equilibrium step (K_1 for ATPγS and K_3 for ATP). This initial binding step is followed by a slow isomerization of the complex (k_2/k_{-2} for ATPγS and k_4/k_{-4} for ATP) to a new conformational state. In the case of ATP, this isomerization is followed by the rapid hydrolysis of ATP and release of ADP and P_i; thus, the observed rate constant for ATP hydrolysis is determined by the rate of the isomerization step. In contrast, the rate of ATPγS hydrolysis is extremely low, and the isomerization is only weakly reversible (see below). As a result, the isomerization step results in an increase in the strength of ATPγS binding in the recA−ssDNA−ATPγS complex. When ATP and ATPγS are both present, they compete for the same catalytic site on the recA protein. At early times, when the rapid equilibrium binding of ATPγS to form the initial complex (E·ATPγS) has been established but before the slow isomerization to the tighter binding state (E*·ATPγS) has occurred, the inhibition by ATPγS is relatively weak, and ATP hydrolysis occurs at a nearly uninhibited rate. As time progresses, however, the slow ATPγS-mediated isomerization of the complex leads to a higher affinity for ATPγS, and the inhibition of the ATP hydrolysis reaction becomes more pronounced. This leads to the slower, steady-state phase of ATP hydrolysis.

In Figure 1, the solid line represents a simulation of the experimental data that was obtained with the model in Scheme 1 and the parameters $K_1 = 55\ \mu$M, $K_3 = 75\ \mu$M, $k_2 = 20\ \text{min}^{-1}$, $k_{-2} = 0.1\ \text{min}^{-1}$, $k_4 = 20.5\ \text{min}^{-1}$, and $k_{-4} = 2\ \text{min}^{-1}$. The adequacy of the fit indicates that the model is sufficient to account for the biphasic time course of the ATPγS-inhibited ATP hydrolysis reaction. Furthermore, the kinetic parameters used to simulate the data are similar to those that were derived for an analogous reaction scheme in our transient fluorescence studies with the [H163W]recA protein (see Experimental Procedures). Thus, the kinetics of the ATPγS-inhibited ATP hydrolysis reaction are consistent with the proposed two-step mechanism for the binding of ATPγS to the recA−ssDNA complex.

Results identical to those shown in Figure 1 were obtained for reactions that were initiated by the addition of recA protein, rather than by addition of ATP and ATPγS. In the latter case, the recA protein is already bound to the ssDNA when the ATP and ATPγS are added, whereas in the former case the free recA protein potentially can interact with ATP or ATPγS before the protein binds to the ssDNA. The equivalence of these results indicates that the binding of recA protein to ssDNA is not kinetically significant in these inhibition experiments. Nevertheless, all experiments in this study were carried out by preincubating the recA protein with ssDNA before either ATP or ATPγS was added (as depicted in Scheme 1) in order to ensure that the recA−ssDNA complex (E) was formed in a consistent way in every experiment.

Dependence of ATPγS Inhibition of ATP Hydrolysis on ATPγS and ATP Concentration. To more critically evaluate the model in Scheme 1, the dependence of the ATPγS inhibition kinetics on ATPγS and ATP concentration was examined. All reactions were initiated by the simultaneous addition of ATP and ATPγS to reaction solutions which contained preformed recA−ssDNA complex.

Time courses of ATP hydrolysis that were obtained at a fixed concentration of ATP (1 mM) and various concentrations of ATPγS (20−60 μM) are shown in Figure 2A. At all ATPγS concentrations examined, the biphasic nature of the time courses was apparent; both the amplitude of the first phase and the rate of the second phase decreased with increasing ATPγS concentration. According to Scheme 1, the dependence of the observed first-order rate constant for the transition from the weakly inhibited to the strongly inhibited state on ATPγS concentration (at a fixed concentration of ATP) is given by eq 1:

$$k_{\text{obs}} = k_2\left(\frac{[\text{ATP}\gamma\text{S}]}{K_1 + K_1[\text{ATP}]/K_3 + [\text{ATP}\gamma\text{S}]}\right) + k_{-2} \quad (1)$$

with $k_{\text{obs}} = k_{-2}$ at zero ATPγS concentration. In Figure 2B, the first-order transition rate constants for the time courses shown in Figure 2A are plotted versus ATPγS concentration; the extrapolated intercept of this plot corresponds to a value of $k_{-2} = 0.13\ \text{min}^{-1}$. Although Eq 1 also predicts that k_{obs} will approach a limiting value of $k_2 + k_{-2}$ at high ATPγS concentration, it was not possible to determine k_2 in this way because at ATPγS concentrations greater than 70 μM the transition to the strongly inhibited state was so fast (and the extent of ATP hydrolysis was so low) that the biphasic time courses could not be measured experimentally.

In Figure 2A, the solid lines represent simulations of the experimental data that were obtained using the model in Scheme 1 and kinetic parameters similar to those used in Figure 1. These results indicate that the model is sufficient to account for the ATPγS concentration dependence of the ATPγS-inhibited ATP hydrolysis reaction that is observed at a fixed concentration of ATP.

Time courses of ATP hydrolysis that were obtained at a fixed concentration of ATPγS (20 μM) and various concentrations of ATP (0.1−1 mM) are shown in Figure 3. At low concentrations of ATP (0.1 mM), the amplitude of the first phase and the rate of the second phase of ATP hydrolysis were both very low, showing that the onset of inhibition is rapid when the ATP concentration is insufficient to allow ATP to compete effectively with ATPγS for binding to the catalytic sites before the tight ATPγS binding state is established [in the absence of ATPγS, the ATP hydrolysis reaction (0.1 mM ATP) proceeded at a rate of 14 $\mu\text{M min}^{-1}$]. As the concentration of ATP was increased, however, ATP was able to compete more effectively with ATPγS in the early stage of the reaction, and the biphasic time course of ATP hydrolysis became apparent. Both the amplitude of the first phase and the rate of the second phase of ATP hydrolysis increased with increasing ATP concentration.

In Figure 3, the solid lines represent simulations of the experimental data that were obtained using the model in

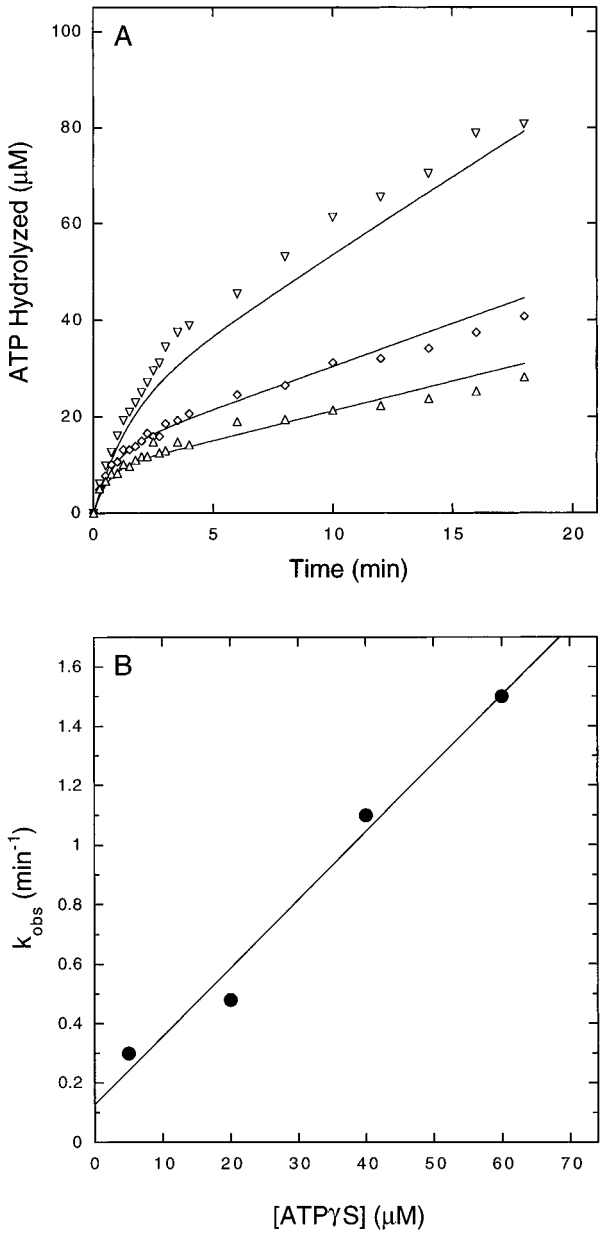

FIGURE 2: Dependence of ATPγS inhibition of ATP hydrolysis on ATPγS concentration. Panel A: Reaction solutions contained 25 mM Tris-HCl (pH 7.5), 10 mM $MgCl_2$, 20 μM dT_{50}, 1 μM [H163W]recA protein, 1 mM [α-^{32}P]ATP, and either 20 μM ($\triangledown$), 40 μM ($\diamond$), or 60 μM ($\triangle$) ATPγS. The reactions were initiated by the simultaneous addition of ATP and ATPγS after incubation of all other components for 8 min at 37 °C. The points represent ATP hydrolyzed as a function of time at 37 °C. The solid line was calculated using the mechanism in Scheme 1 and the parameters $K_1 = 44$ μM, $K_3 = 77$ μM, $k_2 = 19$ min^{-1}, $k_{-2} = 0.13$ min^{-1}, $k_4 = 20.5$ min^{-1}, and $k_{-4} = 2$ min^{-1}. Panel B: Apparent first-order rate constants (k_{obs}) were determined by fitting each of the reaction time courses shown in panel A (plus an additional reaction at 5 μM ATPγS; data not shown) to an exponential process. These rate constants are plotted as a function of ATPγS concentration. The solid line represents a linear fit of the data and extrapolates to a value of $k_{obs} = 0.13$ min^{-1} at zero ATPγS concentration.

Scheme 1 and parameters similar to those used in Figures 1 and 2. These results indicate that the model is sufficient to account for the ATP concentration dependence of the ATPγS-inhibited ATP hydrolysis reaction that is observed at a fixed concentration of ATPγS. Similar results were obtained for a series of ATP hydrolysis time courses that were determined over a range of ATP concentrations (0.1−1

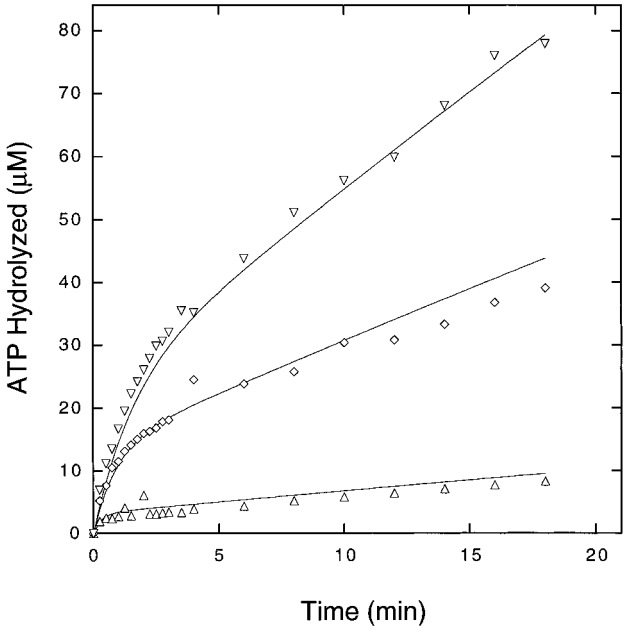

FIGURE 3: Dependence of ATPγS inhibition of ATP hydrolysis on ATP concentration. Reaction solutions contained 25 mM Tris-HCl (pH 7.5), 10 mM $MgCl_2$, 20 μM dT_{50}, 1 μM [H163W]recA protein, 20 μM ATPγS, and either 0.1 mM ($\triangle$), 0.5 mM ($\diamond$), or 1.0 mM ($\triangledown$) [α-^{32}P]ATP. The reactions were initiated by the simultaneous addition of ATP and ATPγS after incubation of all other components for 8 min at 37 °C. The points represent ATP hydrolyzed as a function of time at 37 °C. The solid line was calculated using the mechanism in Scheme 1 and the parameters $K_1 = 47$ μM, $K_3 = 69$ μM, $k_2 = 21$ min^{-1}, $k_{-2} = 0.11$ min^{-1}, $k_4 = 21$ min^{-1}, and $k_{-4} = 2$ min^{-1}.

mM) and an ATPγS concentration of 40 μM (data not shown).

Effect of Preincubation of recA−ssDNA Complexes with ATPγS on the Inhibition of ATP Hydrolysis. In the experiments described thus far, the ATP hydrolysis reactions were started by the simultaneous addition of ATP and ATPγS to the reaction solution. In this case, ATP and ATPγS can immediately compete for binding to the recA−ssDNA complex, and there is a burst of ATP hydrolysis before the ATPγS-mediated isomerization of the complex to the strongly inhibited state occurs. However, the model in Scheme 1 predicts that the kinetics of inhibition will depend on the order of addition of the reaction components. Thus, if the recA−ssDNA complex is first incubated with ATPγS, and the ATP hydrolysis reaction is then initiated by the addition of ATP, the model predicts that there should be a lag in the time course of the ATP hydrolysis reaction because ATPγS would have to dissociate from the recA−ssDNA complex before ATP could compete for binding to the catalytic site. To test this prediction, and to directly measure the reversal of ATPγS inhibition, a series of experiments was carried out using an altered order of addition.

Time courses of ATP hydrolysis that were obtained at a fixed concentration of ATPγS (20 μM) and various concentrations of ATP (1−4 mM) are shown in Figure 4; in these reactions, ATP hydrolysis was initiated by the addition of the indicated concentration of ATP after the reaction solutions containing recA−ssDNA complex and ATPγS (20 μM) had been incubated for 8 min. As predicted, each of the reaction time courses showed a lag before the steady-state phase of ATP hydrolysis was attained. The rate of the steady-state phase increased with increasing ATP concentra-

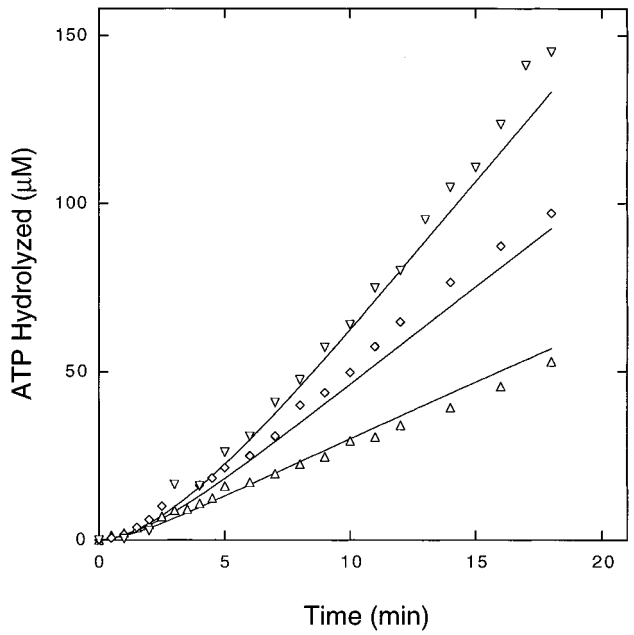

FIGURE 4: Dependence of ATPγS inhibition of ATP hydrolysis on ATP concentration: Lag conditions. Reaction solutions contained 25 mM Tris-HCl (pH 7.5), 10 mM $MgCl_2$, 20 μM dT_{50}, 1 μM [H163W]recA protein, 20 μM ATPγS, and either 1 mM (△), 2 mM (◇), or 4 mM (▽) [α-^{32}P]ATP. The reactions were initiated by the addition of ATP after incubation of all other components (including ATPγS) for 8 min at 37 °C. The points represent ATP hydrolyzed as a function of time at 37 °C. The solid line was calculated using the mechanism in Scheme 1 and the parameters $K_1 = 44$ μM, $K_3 = 77$ μM, $k_2 = 19$ min^{-1}, $k_{-2} = 0.13$ min^{-1}, $k_4 = 21$ min^{-1}, and $k_{-4} = 2$ min^{-1}.

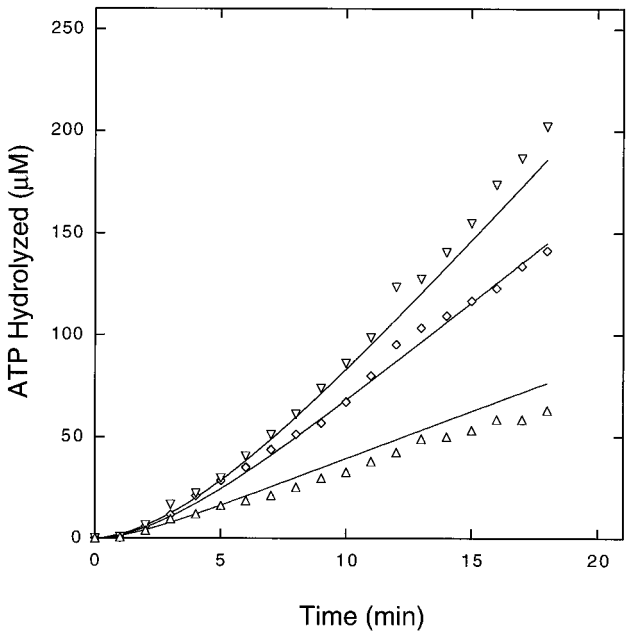

FIGURE 5: Dependence of ATPγS inhibition of ATP hydrolysis on ATPγS concentration: Lag conditions. Reaction solutions contained 25 mM Tris-HCl (pH 7.5), 10 mM $MgCl_2$, 20 μM dT_{50}, 1 μM [H163W]recA protein, 3 mM [α-^{32}P]ATP, and either 10 μM (▽), 20 μM (◇), or 60 μM (△) ATPγS. The reactions were initiated by the addition of ATP after incubation of all other components (including ATPγS) for 8 min at 37 °C. The points represent ATP hydrolyzed as a function of time at 37 °C. The solid line was calculated using the mechanism in Scheme 1 and the parameters $K_1 = 50$ μM, $K_3 = 66$ μM, $k_2 = 19$ min^{-1}, $k_{-2} = 0.13$ min^{-1}, $k_4 = 23$ min^{-1}, and $k_{-4} = 2$ min^{-1}.

tion, indicating that ATP is able to compete more effectively with ATPγS at high ATP concentration. The kinetics of the reactions were independent of the time of the ATPγS preincubation period (over a range from 3 to 15 min), indicating that ATPγS binding had reached equilibrium before the hydrolysis reactions were initiated by the addition of ATP.

In Figure 4, the solid lines represent simulations of the experimental data that were obtained using the kinetic model in Scheme 1 and parameters similar to those used to simulate the time courses that were obtained using the original order of addition (Figures 1−3). These results indicate that the model is sufficient to account for the ATP concentration dependence of the ATPγS-inhibited ATP hydrolysis reaction that is observed when the recA−ssDNA complex is preincubated with a fixed concentration of ATPγS.

Time courses of ATP hydrolysis that were obtained at a fixed concentration of ATP (3 mM) and various concentration of ATPγS (10−60 μM) are shown in Figure 5; in these reactions, ATP hydrolysis was again initiated by the addition of ATP after the reaction solutions containing the recA−ssDNA complex had been incubated with the indicated concentrations of ATPγS for 8 min. All of the time courses exhibited a lag before the steady-state phase of ATP hydrolysis was attained. The rate of the steady-state phase of ATP hydrolysis decreased with increasing ATPγS concentration.

In Figure 5, the solid lines represent simulations of the experimental data that were obtained using the model in Scheme 1 and parameters similar to those used in Figures 1−4. These results indicate that the model is sufficient to account for the ATPγS concentration dependence of the ATPγS-inhibited ATP hydrolysis reaction that is observed when the recA−ssDNA complex is preincubated with a fixed concentration of ATPγS.

Although the nature of the transient phase of the ATPγS-inhibited ATP hydrolysis reaction depended on the order in which the reaction components were added, each of the reactions (at a given concentration of ATP and ATPγS) reached the same final steady-state rate of ATP hydrolysis regardless of the order of addition. This is illustrated in Figure 6A for a pair of reactions each of which contained 20 μM ATPγS and 2 mM ATP but differed in the order of addition. In Figure 6B, the steady-state rate of ATP hydrolysis, as measured at a fixed concentration of ATPγS (20 μM), is plotted as a function of ATP concentration. The double-reciprocal plot extrapolates to the same V_{max} value as does a plot for the ATP hydrolysis reaction in the absence of inhibitor, and is consistent with linear competitive inhibition with an overall K_i for ATPγS of 0.3 μM. This value is consistent with the overall K_i(ATPγS) of 0.3 μM that can be derived from the kinetic parameters that were used to simulate the data in Figures 2−5 [in Scheme 1, the overall $K_i(\text{ATP}\gamma\text{S}) = K_1(k_{-2}/(k_2 + k_{-2}))$]. This confirms that the ATPγS inhibition is due to a reversible binding of ATPγS to the recA−ssDNA complex and not to an irreversible modification or inactivation of the recA protein.

Kinetics of ssDNA-Dependent ATPγS Hydrolysis. Although ATPγS is a poor substrate, it is hydrolyzed by the recA protein at a measurable rate. The hydrolysis of ATPγS and the subsequent dissociation of ADP and thiophosphate could conceivably account (at least partially) for the reversibility of the ATPγS inhibition of the ATP hydrolysis reaction. To investigate this possibility, the steady-state rate

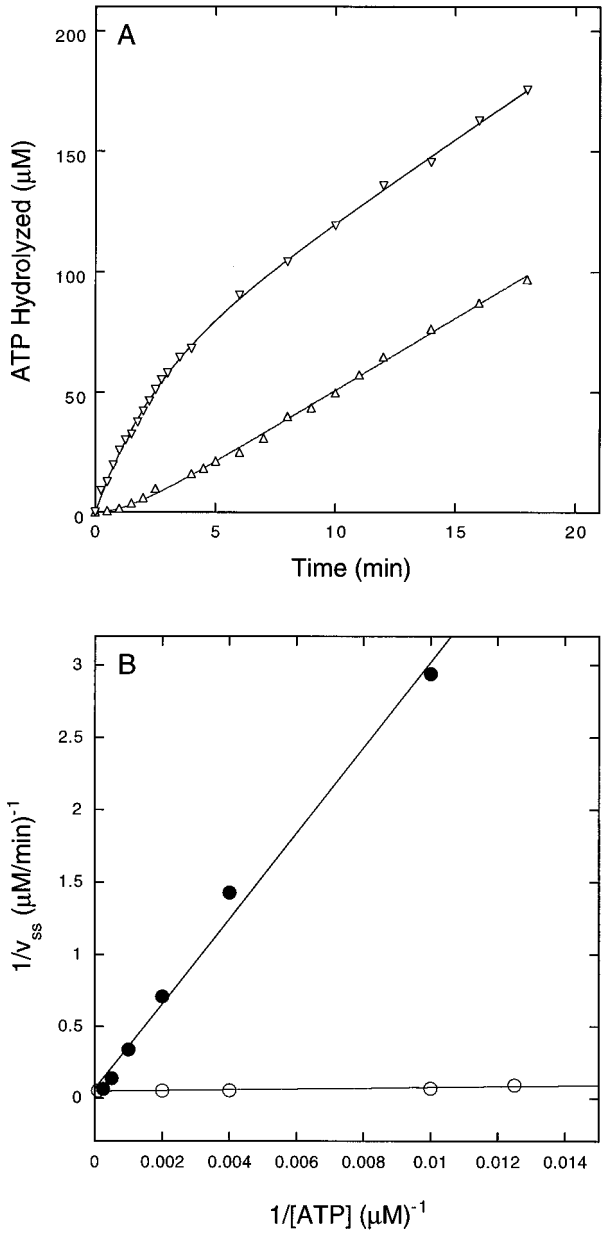

FIGURE 6: Reversibility of ATPγS inhibition of ATP hydrolysis. Panel A: Reaction solutions contained 25 mM Tris-HCl (pH 7.5), 10 mM $MgCl_2$, 20 μM dT_{50}, 1 μM [H163W]recA protein, 2 mM [α-^{32}P]ATP, and 20 μM ATPγS. Reactions were initiated either by the simultaneous addition of ATP and ATPγS ($\triangledown$) or by the addition of ATP ($\triangle$) after incubation of all other components for 8 min at 37 °C. The points represent ATP hydrolyzed as a function of time at 37 °C. Panel B: The final steady-state rates of ATP hydrolysis for reactions containing either 0 μM ($\bigcirc$) or 20 μM ($\bullet$) ATPγS and the indicated concentrations of ATP are presented in the form of a double-reciprocal plot. The solid line represents a fit of the data to the equation for simple linear competitive inhibition (Segel, 1975) and is consistent with $V_{max}/[E_T] = 20$ min^{-1} and K_i(ATPγS) = 0.3 μM.

constant for ATPγS hydrolysis was determined under the conditions of the inhibition experiments described above. The reaction solutions contained 20 μM recA protein and 200 μM dT_{50}, and were carried out at pH 7.5 and 37 °C (note that the concentration of recA protein was higher than in previous experiments so that the rate of the slow ATPγS hydrolysis reaction could be measured accurately).

The time course of ATPγS hydrolysis (500 μM ATPγS) is shown in Figure 7. The reaction followed a linear time course with a steady state rate constant of 0.01 min^{-1}. This

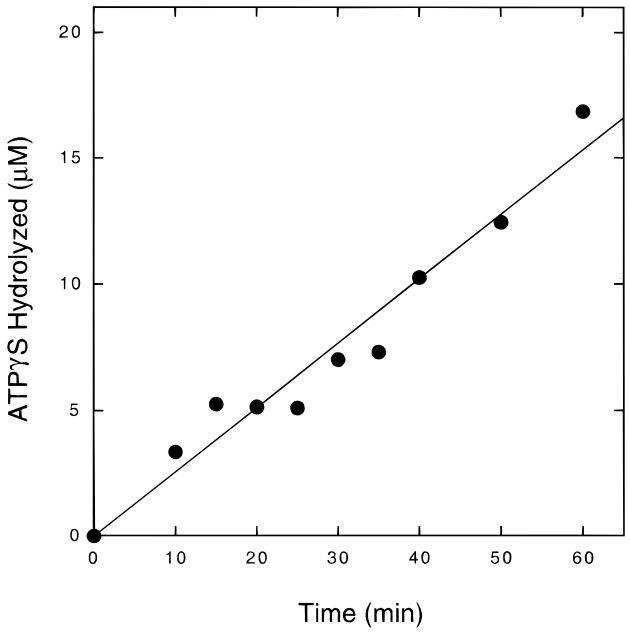

FIGURE 7: Time course of ssDNA-dependent ATPγS hydrolysis. Reaction solutions contained 25 mM Tris-HCl (pH 7.5), 10 mM $MgCl_2$, 200 μM dT_{50}, 20 μM [H163W]recA protein, and 500 μM [γ-^{35}S]ATPγS. The reactions were initiated by addition of recA protein after incubation of all other components for 8 min at 37 °C. The points represent ATPγS hydrolyzed as a function of time at 37 °C.

Scheme 2

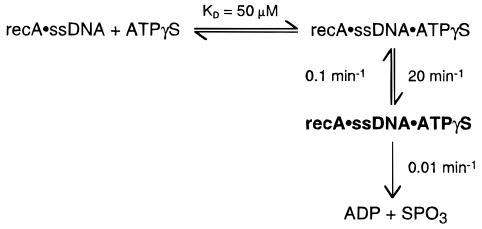

turnover number is nearly 2000-fold lower than that for ATP hydrolysis (20 min^{-1}) under the same conditions (Figure 1). It is also 10-fold lower than the value of $k_{-2} = 0.13$ min^{-1} that was determined in Figure 2B. This indicates that the reversibility of the ATPγS inhibition of ATP hydrolysis is primarily due to the dissociation of ATPγS from the recA−ssDNA−ATPγS complex, and not to ATPγS hydrolysis.

DISCUSSION

The time-dependent inhibition of the recA protein-catalyzed ATP hydrolysis reaction by ATPγS indicates that ATPγS binds to the recA−ssDNA complex by the two-step mechanism shown in Scheme 2. In the first step, ATPγS binds to the recA−ssDNA complex in a rapid equilibrium process ($K_D = 50$ μM). This initial binding step is then followed by a slow isomerization of the complex (20 min^{-1}) to a new conformational state (boldface); the kinetics of inhibition indicate that this isomerization step is only slowly reversible (0.1 min^{-1}). The isomerization step is then followed by the even slower hydrolysis of ATPγS and release of ADP and thiophosphate (0.01 min^{-1}). Because the rate of ATPγS hydrolysis is so low relative to the rate of the isomerization step, and because the isomerization step itself is only weakly reversible, the recA−ssDNA−ATPγS complex is extremely stable. Thus, ATPγS functions as a potent

slow binding inhibitor of the recA protein-catalyzed ATP hydrolysis reaction.[4]

The first-order rate constant for the ATPγS-mediated isomerization step (20 min^{-1}), although significantly greater than the rate of ATPγS hydrolysis (0.01 min^{-1}), is identical to the steady-state rate constant for the recA protein-catalyzed ATP hydrolysis reaction (20 min^{-1}). This suggests that an analogous ATP-mediated isomerization of the recA−ssDNA complex may be the rate-determining step on the ssDNA-dependent ATP hydrolysis reaction pathway. In fact, the kinetic parameters that were used to model the ATPγS inhibition data are very similar to those that were derived for an analogous reaction scheme in our recent transient fluorescence studies on the [H163W]recA protein (see Experimental Procedures). Thus, the ATPγS inhibition results reported here provide strong independent support for the two-step mechanism for the binding of ATP and ATPγS to the recA−ssDNA complex. Furthermore, the results allow us to equate the isomerization of the recA−ssDNA−ATPγS complex to the strongly inhibitory state with the ATPγS-mediated fluorescence change that was observed by stopped-flow fluorescence. Moreover, the results significantly extend our kinetic model by providing a direct measure of both the rate constant for the reversal and the overall equilibrium constant for the ATPγS-mediated isomerization.

It is likely that the ATPγS-mediated isomerization is related to the transition of the recA−ssDNA complex from the strand exchange-inactive closed conformation to the strand exchange-active open conformation. In the simplest case, the first state of the recA−ssDNA−ATPγS complex in Scheme 2 would represent the closed conformation, and the second state would correspond to the open conformation. Our previous transient fluorescence studies, however, indicated that the 20 min^{-1} isomerization step may not correspond directly to the closed to open transition. Instead, the evidence suggests that the 20 min^{-1} isomerization step which follows NTP binding may be either accompanied or rapidly followed by a transition of the complex from the closed to open conformation. In the case of ATP, the 20 min^{-1} isomerization step occurs during every cycle of ATP binding and hydrolysis, whereas the transition from the closed to open conformation may occur only during the first ATP binding event. With ATPγS, however, the rate of hydrolysis is so low that the isomerization of the recA−ssDNA complex that follows ATPγS binding can be considered, to a first approximation, as the final step of the ATPγS binding sequence. In this case, the ATPγS-stabilized open conformational state would represent the strongly inhibitory state of the recA−ssDNA−ATPγS complex.

Although the model in Scheme 1 is sufficient to account for the ATPγS inhibition kinetics reported here, the model is oversimplified in that ATP and ATPγS are depicted as binding to an isolated recA monomer within the recA−ssDNA complex. In fact, ATP binding exhibits positive cooperativity, indicating that the binding of ATP to one recA monomer within the recA−ssDNA complex increases the affinity of a neighboring monomer for ATP. We are currently developing more sophisticated kinetic schemes in an effort to elucidate the role of cooperative interactions in the mechanism of the ATP-mediated transition of the recA−ssDNA complex.

[4] This mechanism may also account for a similar kinetic phenomenon that was noted previously by Lee and Cox (1990; Figure 4).

ACKNOWLEDGMENT

We thank Einar Stole for providing the [H163W]recA protein.

REFERENCES

Brenner, S. L., Mitchell, R. S., Morrical, S. W., Neuendorf, S. K., Schutte, B. C., & Cox, M. M. (1987) *J. Biol. Chem. 262*, 4011−4016.
Bryant, F. R. (1988) *J. Biol. Chem. 263*, 8716−8723.
Cox, M. M. (1994) *Trends Biochem. Sci. 19*, 217−222.
Egelman, E. H. (1993) *Curr. Opin. Struct. Biol. 3*, 189−197.
Frieden, C. (1993) *Trends Biochem. Sci. 18*, 58.
Kowalczykowski, S. C. (1991) *Annu. Rev. Biochem. 20*, 539−575.
Lee, J. W., & Cox, M. M. (1990) *Biochemistry 29*, 7666−7676.
Roca, A. I., & Cox, M. M. (1990) *Crit. Rev. Biochem. Mol. Biol. 25*, 415−456.
Segel, I. H. (1975) *Enzyme Kinetics*, Wiley-Interscience, New York.
Stole, E., & Bryant, F. R. (1994) *J. Biol. Chem. 269*, 7919−7925.
Stole, E., & Bryant, F. R. (1995) *J. Biol. Chem. 270*, 20322−20328.
Stole, E., & Bryant, F. R. (1997) *Biochemistry 36*, 3483−3490.
Weinstock, G. M., McEntee, K., & Lehman, I. R. (1979) *Proc. Natl. Acad. Sci. U.S.A. 76*, 126−130.

BI970576+